GEOPHYSICAL RESEARCH LETTERS, VOL. 37, L02501, doi:10.1029/2009GL041108, 2010

Persistent englacial drainage features in the Greenland Ice Sheet

G. A. Catania[1,2] and T. A. Neumann[3]

Received 26 September 2009; revised 1 December 2009; accepted 30 December 2009; published 29 January 2010.

[1] Surface melting on the Greenland Ice Sheet is common up to ~1400 m elevation and, in extreme melt years, even higher. Water produced on the ice sheet surface collects in lakes and drains over the ice sheet surface via supraglacial streams and through the ice sheet via moulins. Water delivered to the base of the ice sheet can cause uplift and enhanced sliding locally. Here we use ice-penetrating radar data to observe the effects of significant basal melting coincident with moulins and calculate how much basal melt occurred. We find that more melting has occurred than can be explained by the release of potential energy from the drainage of surface meltwater during one melt season suggesting that these moulins are persistent for multiple years. We find only a few persistent moulins in our study area that drain the equivalent of multiple lakes per year and likely remain active over several years. Our observations indicate that once established, these persistent moulins might be capable of establishing well-connected meltwater drainage pathways. **Citation:** Catania, G. A., and T. A. Neumann (2010), Persistent englacial drainage features in the Greenland Ice Sheet, *Geophys. Res. Lett.*, *37*, L02501, doi:10.1029/2009GL041108.

1. Introduction

[2] Surface meltwater on the Greenland Ice Sheet drains overland via supraglacial streams and englacially via moulins [*Das et al.*, 2008; *Catania et al.*, 2008]. Moulins allow for efficient routing of large volumes of supraglacial water to the bed as seen on Arctic polythermal glaciers [*Bingham et al.*, 2008; *Boon and Sharp*, 2003]. Exploration in moulins reveals that they extend englacially through tortuous paths consisting of plunge pools and vertical shafts [*Benn et al.*, 2009; *Vatne*, 2001; *Holmlund*, 1988] and can remain open for several years after they are formed [*Gulley*, 2009]. Moulins in Greenland are thought to form through hydrofracture of water-filled crevasses or lake drainage events [*Alley et al.*, 2005; *Das et al.*, 2008] which may result in short-term increases in surface velocity [*Das et al.*, 2008]. Here we examine moulins previously identified by *Catania et al.* [2008] using ice-penetrating radar data in Greenland near the equilibrium line (69.57 N, 49.33 W) (Figure 1a). Our radar has a wavelength of ~100 m in ice and so we have no way to determine moulin orientation precisely. For this study we hypothesize that moulins are vertical and that water entering through them goes straight to the bed. This is likely a simplification of their more complex geometry. In this paper, we examine the layer stratigraphy surrounding moulins to understand the temporal evolution of the englacial system.

[3] Moulins occur throughout the ablation region and internal layers are visible in all radar profiles with the exception of a portion of our study site (black lines in Figure 1a) where numerous englacial diffractors scatter radar energy. Where internal layers are visible, there is typically no change in layer shape coincident with moulins; with two exceptions (black filled circles along A-A′ and B-B′ (Figure 1a)). In both of these cases, moulins occur where ice flows over a bedrock ridge that spans the downstream region of the surveyed area (Figure 1a) and causes locally elevated tensile stresses [*Catania et al.*, 2008]. These two moulins show similar patterns of layer downwarping; layers are strongly downwarped toward the base of the ice sheet, the deepest visible layer becomes truncated at the bed just upstream of the moulin and layer downwarping is spatially limited, extending 1–5 kilometers downstream (Figure 1). This stratigraphic pattern is typical of localized short-term basal melting resulting from a point source which removes basal ice over a finite region [*Fahnestock et al.*, 2001; *Catania et al.*, 2006; *Leysinger-Vieli et al.*, 2007]. An alternative possibility, that melting occurs as a line source (possibly within a subglacial channel) orthogonal to the radar profile, is ruled out because the diffraction patterns created by moulins are vertically oriented [*Catania et al.*, 2008] and because downwarped layers only occur coincident with moulins. Here we calculate the volume of melt causing layer deformation and estimate moulin closure rates to understand moulin evolution. We hypothesize that localized melting at the ice sheet base is due to the release of potential energy from surface meltwater routed into the moulin.

2. Energy Production and Basal Melt

[4] We use an analytical approach to calculate the amount of basal melting at these two moulins by examining the bright layer that appears ~100 m above the bed in both Figures 1c and 1d. This layer is visible across each radar profile but disappears in the vicinity of each moulin. To quantify melt volume we model this layer in two ways. First, we model the layer geometry in the absence of basal melting using a two-dimensional kinematic ice-flow model described by *Catania et al.* [2006] (black line (Figures 1c and 1d)). Second, we model a melt-influenced layer assuming a Gaussian distribution of basal melting (and thus layer depth) focused at the moulin with a peak and spread that best matches the shape of the observed layer (white line (Figures 1c and 1d)). For Case B (along line B-B′), a double-peaked Gaussian is used. Radar data along line B-B′ were

[1]Institute for Geophysics, University of Texas at Austin, Austin, Texas, USA.
[2]Department of Geology, University of Texas at Austin, Austin, Texas, USA.
[3]Cryospheric Sciences Branch, NASA Goddard Space Flight Center, Greenbelt, Maryland, USA.

0094-8276/10/2009GL041108$05.00

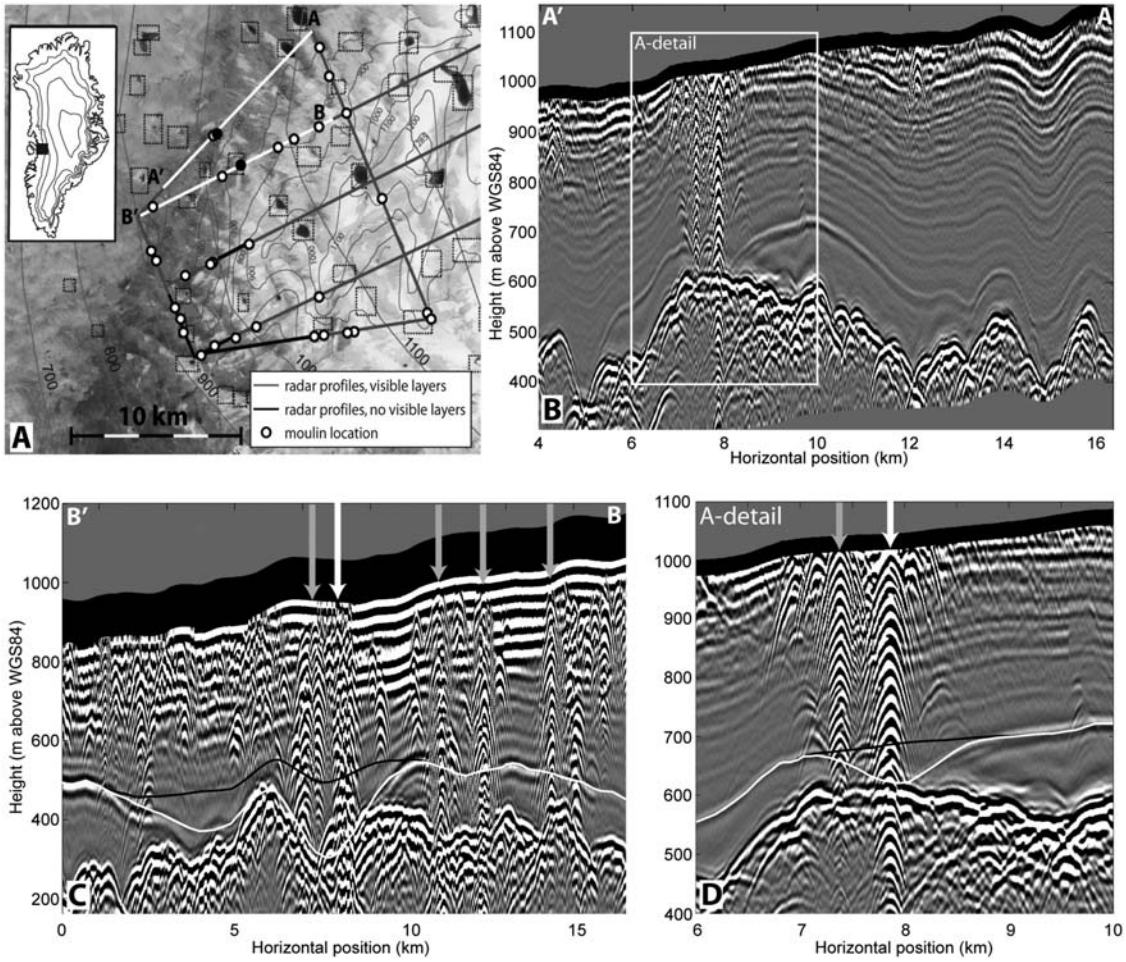

Figure 1. (a) Landsat ETM taken Aug. 1, 2001 showing bed elevation (thin grey contours), surface elevation (thick grey contours) [*Bamber et al.*, 2001], moulin locations (white circles), moulins discussed in the text (black circles), supraglacial lakes (dashed squares) and radar profiles. White lines indicate the location of radar data shown in Figures 1b and 1c. Black lines are regions with no visible internal stratigraphy. (b) The 2 MHz radar profile for the 'Case A' moulin and (c) the 1 MHz radar profile for the 'Case B' moulin. Arrows indicate moulins; white arrows indicate moulins discussed in the text. Modeled (black line) and picked (white line) internal layers are used to calculate melt volume. (d) Detail of line A-A′. Other diffractors in radar are likely from crevasses.

collected along a flow line; data along line A-A′ were not. As a result, we have greater confidence in our modeled layer shapes for Case B than Case A. We subtract the geometry of the melted-influenced layer from the no-melt layer and take the integral of this difference to obtain an estimate of the melted area along each radar profile; 5.8×10^4 m^2 for Case A and 7.8×10^5 m^2 for Case B.

[5] To calculate melt volume we estimate how far melting extends off-axis from our radar profile. We detect moulins up to ~400 m off-axis from our radar profiles (our radar is omni-directional) and so we assume that internal layers are uniformly deformed at least this distance off-axis for each of our two cases; otherwise we would expect to see over-printed layers typical in areas where layer shapes have tight folds in three-dimensions [*Harrison*, 1971]. For Case A, we assume a radially-symmetric Gaussian-shaped melt pattern centered on the moulin with a radius of 400 m yielding a melt volume of 1.4×10^7 m^3. For Case B, we use a Gaussian melt distribution that extends off-axis from the radar profile 400 m and 10 km along the radar profile (using the double-peaked melt distribution described above) to yield a melt volume of 1.1×10^8 m^3. Our melt volume estimates are relatively insensitive to the depth accuracy of radar-detected internal layers. If our layers are accurate to ±10 m this introduces a ±10% uncertainty in our volume estimates. Our assumptions regarding the three-dimensional shape of the melted volume induce larger uncertainty because melt extent off-axis from the radar profile is not well constrained. Changing the lateral melt extent by a factor of 2 introduces a ±50% uncertainty in the volume estimates, yielding a combined uncertainty of ±60%.

[6] The energy required to melt a volume of ice is given by $E_m = V_i \rho_i L_i$ where V_i is the ice volume, ρ_i is the ice density (910 kg m^{-3}) and L_i is the latent heat of fusion for ice (3.3×10^5 J kg^{-1}). Our volume estimates require $E_m = 4.2 \times 10^{15}$ J for Case A and 3.3×10^{16} J for Case B. We generate a minimum estimate of the energy required by assuming that the ice sheet base is at the pressure melting point (based on borehole temperatures recorded just north of Jakobshavn Isbrae [*Lüthi et al.*, 2002]), no energy is lost

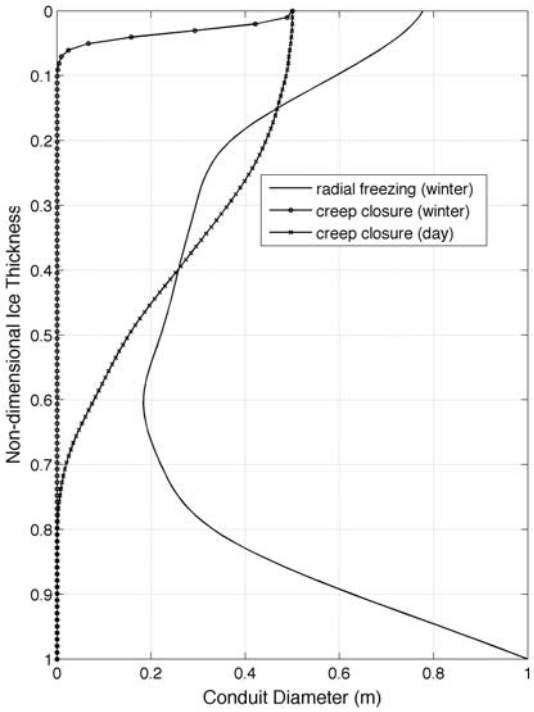

Figure 2. Changes in moulin diameter calculated for a 1 m wide cylindrical conduit based on inward freezing (solid line) and creep closure over 9 months (dashed line) and creep closure over 1 day (dotted line).

through transport of water supraglacially, no energy is required to create or enlarge the moulin, and no energy is lost during subglacial water flow. In other words, all available energy in the surficial melt water is used to melt ice directly at the base of the moulin. We examine the amount of energy supplied via supraglacial lake drainage and then for supraglacial streams.

[7] We calculate the total available energy as the sum of the gravitational potential energy and thermal energy due to the temperature difference between lake water and the basal ice temperature. The basal ice temperature is taken to be 0.3°C for Case A and 0.4°C for Case B based on a melting-point depression of 0.074°C MPa^{-1} [*Paterson*, 1994]. The largest supraglacial lake formed in the Swiss Camp region from 2000–2005 was 5.3×10^7 m^3 [*Box and Ski*, 2007]. The gravitational potential energy released during a lake discharge event is given by $E_l = V_w \rho_w g H$ where V_w is the water volume, ρ_w is the water density, g is the acceleration due to gravity and H is the ice thickness (423 m in Case A and 630 m in Case B). The thermal energy supplied by a lake is given by $E_T = cV_w\rho_w dT$ where c is the specific heat capacity of water (4186 J kg^{-1} $°C^{-1}$) and dT is the temperature difference between the lake and the ice at the bed. Using a lake temperature of 0°C we calculate $E_T = 0.7 \times 10^{14}$ and 0.9×10^{14} for Case A and B respectively and a total energy supply of 2.9×10^{14} J for Case A and 4.2×10^{14} J for Case B. As a lower bound, a single large lake drainage event can melt $\sim 7 \times 10^5$ m^3 of ice and would produce only a few meters dip in internal layers, which would be undetectable with our radar system. Thus, those moulins without noticeably dipping internal layers may have only a temporary connection to the subglacial system or may simply be deep crevasses. As an upper bound, if the total lake volume from the Swiss Camp region ($\sim 3.8 \times 10^8$ m^3 between July 7 and August 1, 2001 [*McMillan et al.*, 2007]) drained into a single moulin the total amount of subglacial melt for Case A can be fully explained.

[8] A single lake drainage event cannot provide adequate energy to explain the observed melt volumes. It would take $\sim 14 \pm 8$ similarly-sized lake drainage events to create the layer pattern observed for Case A and $\sim 78 \pm 47$ for Case B. These estimates are highly sensitive to the temperature of supraglacial lake water; every 3°C increase in lake temperature results in a $1/e$ decrease in the number of lakes required to produce the dipping layers. Thus, a lake temperature of 3°C reduces the number of lakes to 5 and 29 for Cases A and B, respectively. Water may also be supplied via supraglacial streams which contain water at temperatures typically much cooler than lakes (up to ~0.2°C [*Isenko et al.*, 2005]) and so provide no thermal energy. If we assume a supraglacial stream discharge of ~ 2 $m^3 s^{-1}$ [*Bingham et al.*, 2008] we find that the stream would need to run continuously for 16 ± 9 and 84 ± 49 years to melt the ice in Case A and Case B, respectively. Some combination of lake drainage and surface melt runoff supplied to the moulins will reduce the overall streamflow duration or the number of lake drainages required to create the observed layer pattern. However, we argue that these two moulins are necessarily re-activated each summer for multiple years or they drain significantly larger catchment regions than a single lake basin.

3. Moulin Closure Timescale

[9] We calculate moulin closure rates assuming a cylindrical, vertically-oriented moulin. A moulin is expected to close due to inward freezing if it is water-filled, and radial ice creep if it is air-filled or if the water pressure in the moulin is less than the surrounding ice pressure. Additionally, since ice in this region is deforming in simple shear, ice deformation will act to close both water and air-filled moulins. We suspect that moulins can remain water-filled if they become isolated from the subglacial drainage system. If we assume that water in a moulin is at the local depth-dependent pressure-freezing temperature, T_w, then the layer thickness of ice frozen onto the side walls of the moulin over time t is given by

$$d(t) = \frac{C(T_w - T_i)}{\sqrt{\pi} L_i} 2\sqrt{\kappa t} \quad (1)$$

[*Alley et al.*, 2005] where $C = 2093$ J $kg^{-1}K^{-1}$ is the heat capacity, T_i is the ice temperature and $\kappa = 37.2$ $m^2 a^{-1}$ is the thermal diffusivity of ice. We assume that freezing occurs between the beginning of September and June (9 months) because positive degree days are near or equal to zero during these times in our study area [*Zwally et al.*, 2002]. Using equation (1) and T_i from borehole temperature data adjusted for local ice thickness [*Lüthi et al.*, 2002] we find that a 1 m wide moulin will not completely freeze in 9 months (Figure 2). We neglect freezing of surface water within a moulin during winter but estimate that this would produce a ~1.1 m plug of ice at the surface based on a

maximum temperature difference of ~30°C between the water and air temperature at the moulin.

[10] To estimate the radial closure of an air-filled conduit we estimate the change in radius of a conduit subject to creep closure under gravity [*Paterson*, 1977; *Nye*, 1953] using

$$\dot{\epsilon}(a) = -(t)^{-1} \ln(r_f/r_i) \quad (2)$$

where r_i and r_f are the initial and final moulin radii respectively and $\dot{\epsilon}$ is given by Glen's flow law [*Glen*, 1958]. We find that an air-filled moulin with an initial diameter of 1 m will close due to creep very quickly (a few days) with the greatest closure rates at the ice sheet base (Figure 2). Internal deformation measured in a nearby borehole [*Lüthi et al.*, 2002] was found to be negligible in the top 80% of the ice thickness suggesting that only the lower 20% of a water-filled moulin would close through ice deformation over winter. It would therefore take additional energy to re-establish the subglacial connection each year. Based on these estimates we argue that water-filled moulins can remain open over 80% of their lengths as long as the initial diameter is greater than ~1 m.

4. Discussion

[11] Surface lakes appear to be spatially fixed [*Echelmeyer et al.*, 1991; *Box and Ski*, 2007] indicating that they may be controlled by bed topography; the lake associated with the moulin in Case B occurs in a bedrock depression as do other lakes (e.g., at 15 km in Figure 1b). Further, lakes are perpetuated yearly due to an albedo feedback in which the dark water locally increases surface melting and enhances the lake basin [*Luthje et al.*, 2006]. The bed also exerts strong control on moulin locations, which appear to be well-correlated to regions of elevated along-flow tensile stresses [*Catania et al.*, 2008]. Further, moulins and lakes are not always coincident [*Catania et al.*, 2008]. However, both the englacial and supraglacial drainage systems must advect with ice flow. Thus the evolution of the englacial drainage system may be somewhat analogous to the headward migration of nickpoints in bedrock river systems which form spontaneously due to channel bed irregularities, changes in base level or lithology [*Whipple*, 2004]. On ice, nickpoints mark the location where moulins initiate. Advection of ice precludes headward migration of nickpoints and the englacial and supraglacial system is moved downstream until it can no longer be maintained (i.e., the moulin is cut off from the supra- or subglacial water system possibly by a new crevasse opening upstream of the existing moulin). We expect that a new moulin will form in the location where bed topographic conditions are favorable for crevassing, likely in the same location as the one formed previously. If we assume a regional velocity of ~90 m a^{-1} [*Zwally et al.*, 2002] it would take ~44 years for these moulins to advect out of the region of extension (~4 km wide [*Catania et al.*, 2008]) in which they currently reside. We suspect that this lifetime is an upper limit because our observations indicate that moulins are spaced ~1 km apart, indicating a lifetime of ~11 years.

[12] In our survey area, moulins are visible up to 400 m off-axis from our radar profiles which means that the radar data represent an 800 m swath of ice across the profiling direction along each radar profile. We collected a cumulative length of ~105 km of radar profiles suggesting that our data represent coverage of ~37% of the survey area shown in Figure 1a. The discovery of these two persistent moulins suggests the presence of an additional 5–6 persistent moulins within the entire survey area. Despite the formation of numerous moulins, most of them are not associated with dipping internal layers implying that the supraglacial drainage system establishes a long-term connection to only a few moulins as ice is advected downstream. This might occur if the supraglacial drainage pathways are deep enough to make it difficult for water to re-route [e.g., *Gulley et al.*, 2009] or if the moulin was located directly beneath a supraglacial lake that re-forms each year and advects downstream with the moulin. Englacial drainage can also occurs through a network of smaller englacial cracks [*Fountain et al.*, 2005] and this may be the dominant drainage mechanism in the downstream region of our survey area where numerous englacial diffractors prevent observations of englacial stratigraphy. The persistence of these moulins suggests that once a well-developed englacial and supraglacial conduit system is established it is capable of consistently delivering large volumes of surface meltwater to the subglacial system. Greater efficiency of the drainage system may limit the spatial and temporal effect that lake drainage events have on surface velocities as observed in Greenland [*Das et al.*, 2008].

[13] **Acknowledgments.** We thank VECO, J. Greenbaum and J. Rumrill for assistance in the field. S. Price, B. Bindschadler, two anonymous reviewers, and our editor provided comments that substantially improved the manuscript. This work was supported by NASA (grant NNG06GA83G).

References

Alley, R., T. Dupont, B. Parizek, and S. Anandakrishnan (2005), Access of surface meltwater to beds of sub-freezing glaciers: Preliminary insights, *Ann. Glaciol.*, *40*, 8–14.

Bamber, J., S. Ekholm, and W. Krabill (2001), A new, high resolution digital elevation model of Greenland fully validated with airborne laser altimeter data, *J. Geophys. Res.*, *106*(B4), 6733–6745.

Benn, D., J. Gulley, A. Luckman, A. Adamek, and P. Glowacki (2009), Englacial drainage systems formed by hydrologically driven crevasse propagation, *J. Glaciol.*, *55*(191), 513–523.

Bingham, R. G., A. L. Hubbard, P. W. Nienow, and M. J. Sharp (2008), An investigation into the mechanisms controlling seasonal speedup events at a High Arctic glacier, *J. Geophys. Res.*, *113*, F02006, doi:10.1029/2007JF000832.

Boon, S., and M. Sharp (2003), The role of hydrologically-driven ice fracture in drainage system evolution on an Arctic glacier, *Geophys. Res. Lett.*, *30*(18), 1916, doi:10.1029/2003GL018034.

Box, J., and K. Ski (2007), Remote sounding of Greenland supraglacial melt lakes: implications for subglacial hydraulics, *J. Glaciol.*, *53*(181), 257–265.

Catania, G. A., H. Conway, C. F. Raymond, and T. A. Scambos (2006), Evidence for floatation or near floatation in the mouth of Kamb Ice Stream, West Antarctica, prior to stagnation, *J. Geophys. Res.*, *111*, F01005, doi:10.1029/2005JF000355.

Catania, G., T. Neumann, and S. Price (2008), Characterizing englacial drainage in the ablation zone of the Greenland Ice Sheet, *J. Glaciol.*, *54*(187), 567–578.

Das, S., I. Joughin, M. Behn, I. Howat, M. King, D. Lizarralde, and M. Bhatia (2008), Fracture propagation to the base of the Greenland Ice Sheet during supraglacial lake drainage, *Science*, *320*, 778–781, doi:10.1126/science.1153360.

Echelmeyer, K., T. Clarke, and W. Harrison (1991), Surficial glaciology of Jakobshavns Isbræ, West Greenland. I: Surface morphology, *J. Glaciol.*, *37*(127), 368–382.

Fahnestock, M., W. Abdalati, S. Luo, and S. Gogineni (2001), Internal layer tracing and age-depth-accumulation relationships for the northern Greenland ice sheet, *J. Geophys. Res.*, *106*(D24), 33,789–33,797.

Fountain, A., R. Jacobel, R. Schlichting, and P. Jansson (2005), Fractures as the main pathways of water flow in temperate glaciers, *Nature*, *433*(7026), 618–621.

Glen, J. W. (1958), The flow law of ice. A discussion of the assumptions made in glacier theory, their experimental foundations and consequences, *Int. Assoc. Sci. Hydrol.*, *47*, 171–183.

Gulley, J. (2009), Structural control of englacial conduits in the temperate Matanuska Glacier, Alaska, USA, *J. Glaciol.*, *55*(192), 681–690.

Gulley, J., D. Benn, D. Muller, and A. Luckman (2009), A cut-and-closure origin for englacial conduits in uncrevassed regions on polythermal glaciers, *J. Glaciol.*, *55*(189), 66–80.

Harrison, C. (1971), Radio-echo sounding: Focusing effects in wavy strata, *Geophys. J. R. Atron. Soc.*, *24*, 383–400.

Holmlund, P. (1988), Internal geometry and evolution of moulins, Storglaciären, Sweden, *J. Glaciol.*, *34*(117), 242–248.

Isenko, E., R. Naruse, and B. Mavlyudov (2005), Water temperature in englacial and supraglacial channels: Change along the flow and contribution to ice melting on the channel wall, *Cold Reg. Sci. Technol.*, *42*, 53–62.

Leysinger-Vieli, G.-M., R. Hindmarsh, and M. Siegert (2007), Three-dimensional flow influences on radar layer stratigraphy, *Ann. Glaciol.*, *46*, 22–28.

Lüthi, M., M. Funk, A. Iken, S. Gogineni, and M. Truffer (2002), Mechanisms of fast flow in Jakobshavns Isbræ, Greenland. Part III: Measurements of ice deformation, temperature and cross-borehole conductivity in boreholes to the bedrock, *J. Glaciol.*, *48*(162), 369–385.

Luthje, M., L. Pedersen, N. Reeh, and W. Greuell (2006), Modelling the evolution of supraglacial lakes on the West Greenland ice-sheet margin, *J. Glaciol.*, *52*(179), 608–618.

McMillan, M., P. Nienow, A. Shepherd, T. Benham, and A. Sole (2007), Seasonal evolution of supra-glacial lakes on the Greenland Ice Sheet, *Earth Planet. Sci. Lett.*, *262*, 484–492.

Nye, J. F. (1953), The flow law of ice from measurements in glacier tunnels, laboratory experiments and the Jungfraufirn borehole experiment, *Proc. R. Soc. London, Ser. A*, *219*(1193), 477–489.

Paterson, W. S. B. (1977), Secondary and tertiary creep of glacier ice as measured by borehole closure rates, *Rev. Geophys.*, *15*(1), 47–55.

Paterson, W. S. B. (1994), *The Physics of Glaciers*, 3rd ed., 480 pp., Elsevier, Oxford, U. K.

Vatne, G. (2001), Geometry of englacial water conduits, Austre Broggerbreen, Svalbard, *Norw. J. Geogr.*, *55*(2), 85–93.

Whipple, K. X. (2004), Bedrock rivers and the geomorphology of active orogens, *Annu. Rev. Earth. Planet. Sci.*, *32*(1), 151–185, doi:10.1146/annurev.earth.32.101802.120356.

Zwally, H., W. Abdalati, T. Herring, K. Larson, J. Saba, and K. Steffen (2002), Surface melt-induced acceleration of Greenland Ice-Sheet flow, *Science*, *297*(5579), 218–222.

G. A. Catania, Institute for Geophysics, University of Texas at Austin, 10100 Burnet Rd., Austin, TX 78759, USA. (gcatania@ig.utexas.edu)

T. A. Neumann, Cryospheric Sciences Branch, NASA Goddard Space Flight Center, Code 614.1, Greenbelt, MD 20771, USA.